ACS APPLIED MATERIALS & INTERFACES

Research Article

www.acsami.org

Sulfonated Polyimide/Acid-Functionalized Graphene Oxide Composite Polymer Electrolyte Membranes with Improved Proton Conductivity and Water-Retention Properties

Ravi P. Pandey,[†,‡] Amit K. Thakur,[†] and Vinod K. Shahi*[,†,‡]

[†]Electro-Membrane Processes Division and [‡]Academy of Scientific and Innovative Research, Central Salt and Marine Chemicals Research Institute, Council of Scientific & Industrial Research, Gijubhai Badheka Marg, Bhavnagar 364 002, Gujarat, India

Supporting Information

ABSTRACT: Sulfonated polyimide (SPI)/sulfonated propylsilane graphene oxide (SPSGO) was assessed to be a promising candidate for polymer electrolyte membranes (PEMs). Incorporation of multifunctionalized (-SO_3H and -COOH) SPSGO in SPI matrix improved proton conductivity and thermal, mechanical, and chemical stabilities along with bound water content responsible for slow dehydration of the membrane matrix. The reported SPSGO/SPI composite PEM was designed to promote internal self-humidification, responsible for water-retention properties, and to promote proton conduction, due to the presence of different acidic functional groups. Strong hydrogen bonding between multifunctional groups thus led to the presence of interconnected hydrophobic graphene sheets and organic polymer chains, which provides hydrophobic−hydrophilic phase separation and suitable architecture of proton-conducting channels. In single-cell direct methanol fuel cell tests, SPI/SPSGO-8 exhibited 75.06 mW·cm^{-2} maximum power density (in comparison with commercial Nafion 117 membrane, 62.40 mW·cm^{-2}) under 2 M methanol fuel at 70 °C.

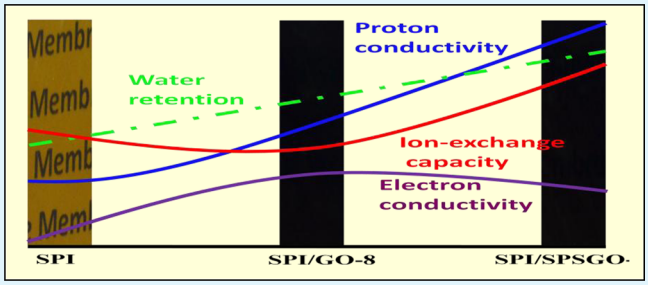

KEYWORDS: *sulfonated graphene oxide, sulfonated polyimide, polymer electrolyte membranes, improved water-retention properties, direct methanol fuel cell*

INTRODUCTION

Advanced nanostructured materials for energy applications, such as water splitting, hydrogen pumps, fuel cells, batteries, and other electrochemical devices, require polymer electrolyte membranes (PEMs) with high proton conduction, chemical stability, and electron insulation.[1,2] Direct methanol fuel cells (DMFCs) provide an attractive alternative to rechargeable batteries in electronic devices because of high efficiency, long lifetimes, ability to refuel, operation at moderate temperatures, and low emission.[3−7] For DMFC applications, PEMs should exhibit several demanding properties, such as good mechanical, thermal, and chemical stabilities, high proton conductivity, and imperviousness toward methanol.[7−9] Generally, perfluorosulfonated polymers, such as DuPont's Nafion membrane, are considered as a benchmark due to their desired properties.[10−15] Several practical drawbacks of perfluorosulfonated membranes, such as high methanol permeability, deterioration in proton conductivity above 100 °C, cost, and environmental inadaptability, led to serious efforts to develop alternative PEMs, especially sulfonated aromatic polymers.[8,9,16] Among the sulfonated aromatic polymers, sulfonated polyimides (SPIs) were considered as promising alternative materials because of their high stabilities (thermal and mechanical), good film-forming ability, low cost, and low fuel crossover.[17−20]

In SPIs, hydrolysis of imide groups occurs due to nucleophilic attack on the carbonyl carbon atoms under fuel cell operating conditions. However, dianhydrides with a high electron density in the carbonyl carbon atoms produced hydrolytically stable and nucleophilic attack-resistant polyimides.[21] Recently, we reported aliphatic−aromatic sulfonated polyimide and acid-functionalized polysilsesquioxane composite membranes.[21] The possibility of incorporating graphene oxide (GO) (potential proton transport vehicle) in SPI matrix was also explored, as GO contains different functional groups (-O-, -OH, -COOH) responsible for hydrogen bonding with SPI and formation of proton conducting channels.[22−24]

Polymer/GO composites are attractive materials for potential applications in supercapacitors, photovoltaic devices, actuators, and biosensors.[25−30] GO is exfoliated from graphite oxide (GtO), prepared by oxidation of graphite by modified Hummers method. GO provides a more facile environment for proton conduction, by a "hopping" mechanism, and enhanced water-retention properties of composite PEM (necessary for proton conduction in nonhumid conditions), because of its large surface area and the presence of hydrophilic

Received: July 14, 2014
Accepted: September 10, 2014
Published: September 10, 2014

Scheme 1. Preparation of Sulfonated Propylsilane Graphene Oxide

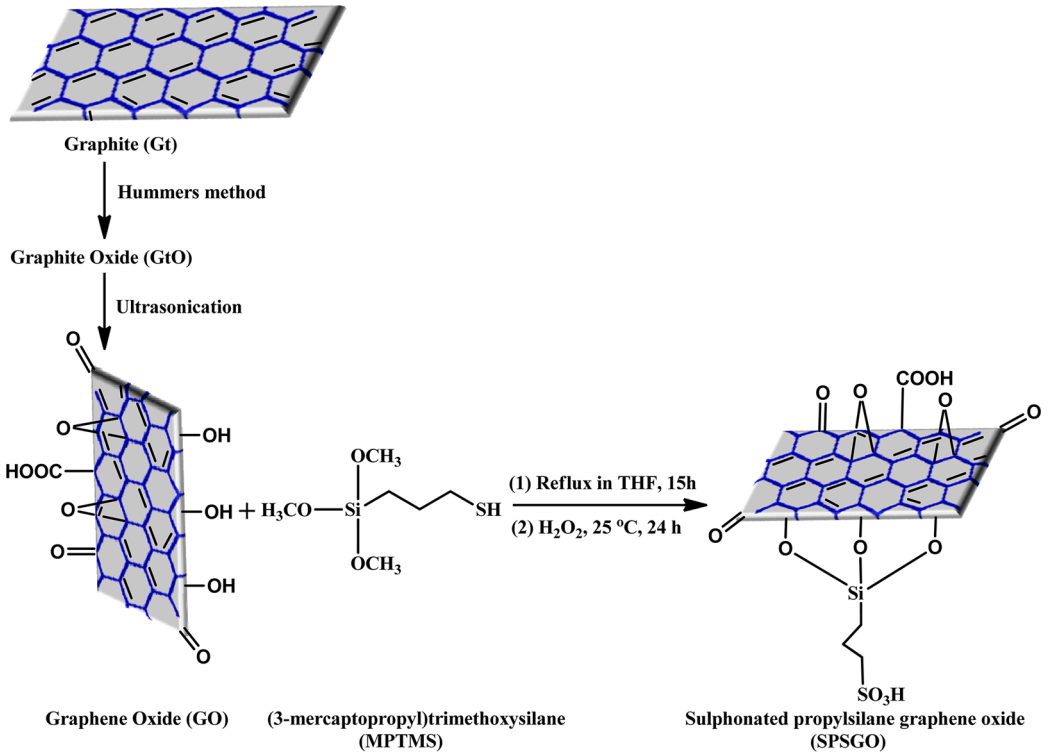

functional groups. Thus, GO was considered as an attractive organic filler in PEM, because its incorporation enhances proton conductivity and water retention and provides an electron-insulating environment.[22,31] But these properties of GO could be further improved after acid functionalization by grafting of sulfonic acid groups. Although free-standing sulfonated GO has been reported with 0.04 $S \cdot cm^{-1}$ proton conductivity at 303 K, its mechanical stability is a serious concern.[32] Furthermore, incorporation of sulfonated GO in sulfonated polymer matrix (SPI) is expected to improve the proton conductivity (high concentration of sulfonic acid groups) along with water-retention and mechanical properties of the PEM.[33,34]

Herein, we report a sulfonated propylsilane graphene oxide (SPSGO)/SPI composite membrane with improved proton conductivity, water retention, and mechanical properties for DMFC applications. Strong interactions between SPI and SPSGO were responsible for homogeneous dispersion with hydrophobic−hydrophilic phase separation, and thus formation of proton-conducting channels. Aliphatic−aromatic sulfonated polyimide, previously reported by our laboratory, was chosen because of its hydrolytically stable and nucleophilic attack-resistant nature.[21]

EXPERIMENTAL SECTION

Materials. Graphite (Gt) powder (size 100 μm) was purchased from SD Fine Chemicals India. Benzophenone-3,3′,4,4′-tetracarboxylic dianhydride (BTCDA), (3-mercaptopropyl)trimethoxysilane (MPTMS), and 1,4-diaminobutane (DAB) (99%) were received from Aldrich. Dimethylacetamide (DMAc), tetrahydrofuran (THF), triethylamine (TEA), benzoic acid, *m*-cresol, acetone, $NaNO_3$, $KMnO_4$, H_2O_2, H_2SO_4, HCl, NaOH, methanol, and NaCl of analytical reagent (AR) grade were obtained from SD Fine Chemicals India and used with proper purification. Other chemicals are of commercial grade and used as received. In all experiments, Milli-Q water was used. 4,4′-Bis(4-aminophenoxy)biphenyl-3,3′-disulfonic acid (BAPBDS) was synthesized from 4,4′-bis(4-aminophenoxy)biphenyl (BAPB) (>97%, TCI) according to the procedure reported earlier.[7]

Preparation of Graphene Oxide. Graphite oxide (GtO) was synthesized by the modified Hummers method from purified natural flake graphite (Gt) powder. A 500 mL round-bottom flask was charged with Gt (2.0 g), $NaNO_3$ (2.0 g), and H_2SO_4 (96 mL) and kept in an ice bath. $KMnO_4$ (6.0 g) was added gradually under stirring below 20 °C. Gradually, reaction temperature was increased to 35 ± 3 °C for 30 min and then to 95 ± 3 °C for 30 min, followed by slow addition of H_2O (180 mL). The reaction was terminated by addition of a large amount of distilled water. Further 30% H_2O_2 solution was added to neutralize the excess amount of permanganate. Finally, the mixture was centrifuged and the precipitate was washed with 5% aqueous HCl solution, and water. The final precipitate was dried overnight under vacuum. GO was exfoliated from GtO by ultrasonication.[30]

Preparation of Sulfonated Propylsilanegraphene Oxide, Sulfonated Polyimide, and Membrane. In a typical preparation procedure for SPSGO (Scheme 1), GO (10 mg), MPTMS [100 mg (in 10:1 MPTMS/GO)], and anhydrous THF (100 mL) were added to a three-neck round-bottom flask equipped with a magnetic stir bar and condenser. The resulting mixture was refluxed at 60 °C for 15 h. Then the reaction mixture was cooled to room temperature and THF was removed by filtration. The obtained filtrate was treated with 30 wt % H_2O_2 solution at 25 °C (24 h) for oxidation of mercapto groups. Finally, the oxidized product was filtered, washed with water/methanol, and dried overnight under vacuum.[31,35] Sulfonated polyimide (SPI) was prepared by our laboratory method described earlier.[21]

Membranes were prepared by solution casting method. In a typical procedure, a known amount of SPSGO (0−8 wt % relative to the SPI) was homogeneously dispersed in DMAc (100 mL) under sonication, a known amount of SPI (20% w/v) was added to the solution, and the resulting mixture was stirred for 24 h at room temperature. The obtained highly viscous solution was cast as a thin film on a cleaned glass plate and dried in a vacuum oven at 80 °C for 12 h. A schematic route for preparation of these composite membranes is depicted in

Scheme 2. Schematic Route for Preparation of SPI/SPSGO Composite Membranes

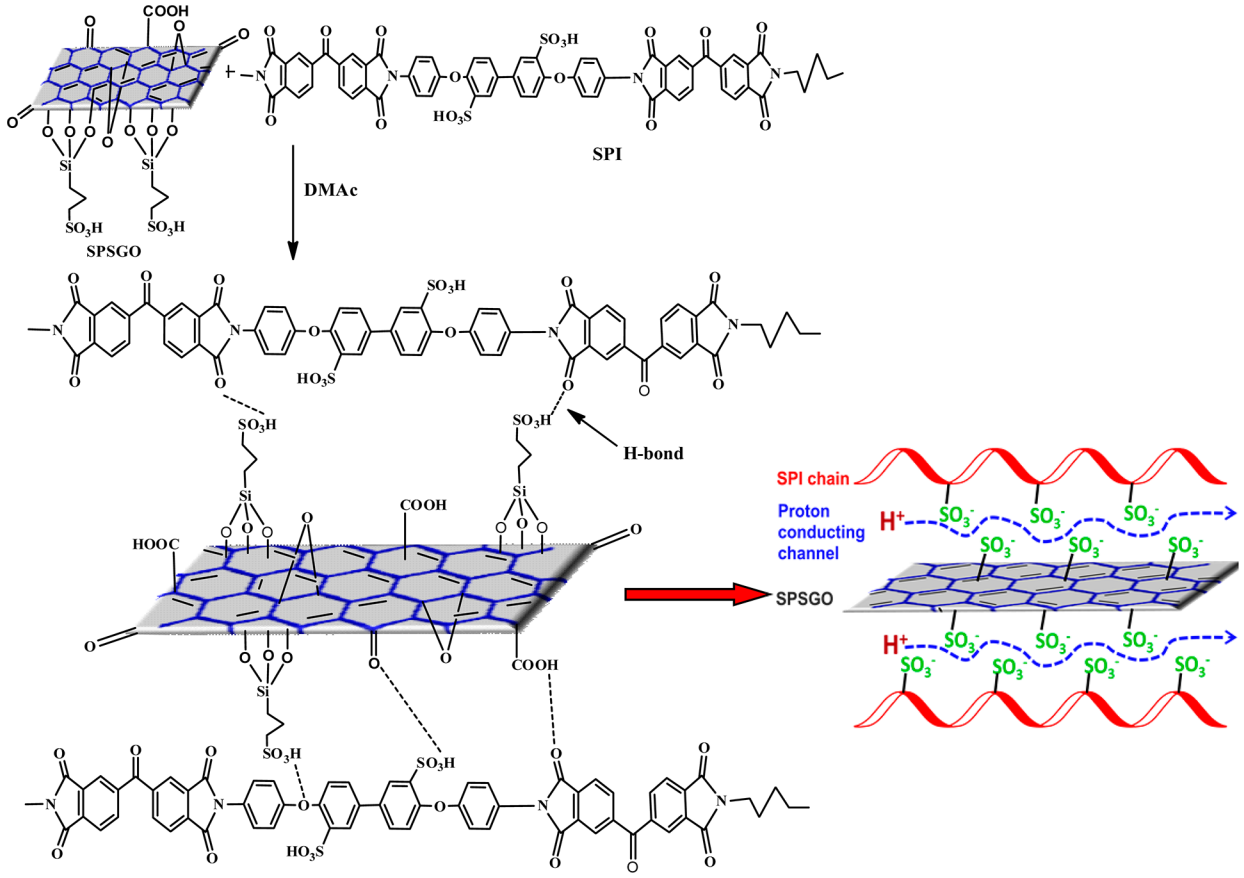

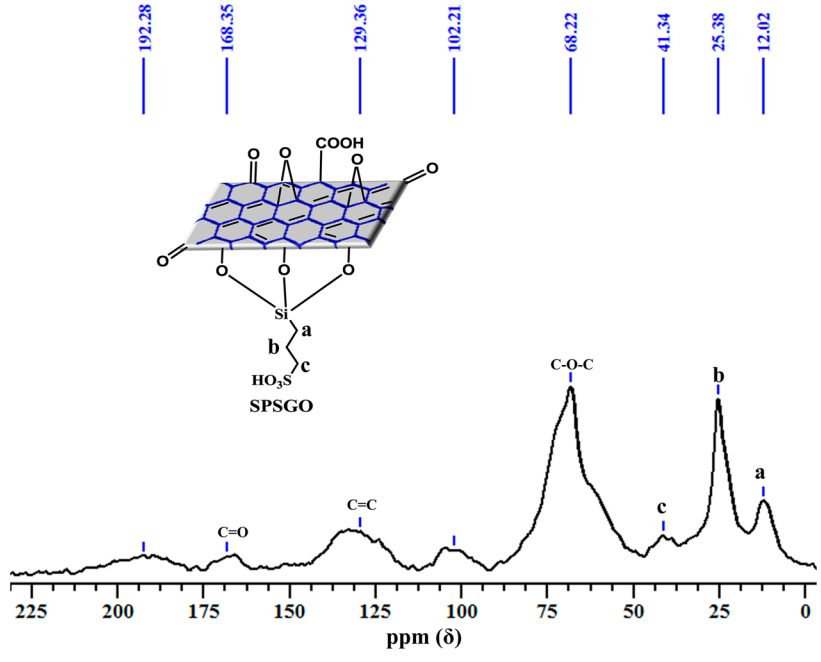

Figure 1. Solid-state ^{13}C NMR spectrum of SPSGO.

Scheme 2. Prepared membranes were designated as SPI/SPSGO-X, where X is the weight percentage of SPSGO (0, 4, 6, or 8 wt %).

Instrumental Analysis. Detailed instrumental analysis such as IR spectra, solid-state ^{13}C NMR spectra, wide-angle X-ray diffraction (XRD), transmission electron microscopy (TEM), scanning electron microscopy (SEM), optical images, thermogravimetric analysis (TGA), and dynamic mechanical analysis (DMA) are included in section S1 of Supporting Information. Bound water content was estimated from weight loss percentage obtained by sample heating in TGA with 10 °C·min^{-1} rate under nitrogen atmosphere between 100 and 150 °C.[36]

Water Uptake, Ion-Exchange Capacity, and Stability Measurements. Detailed procedures for determination of water

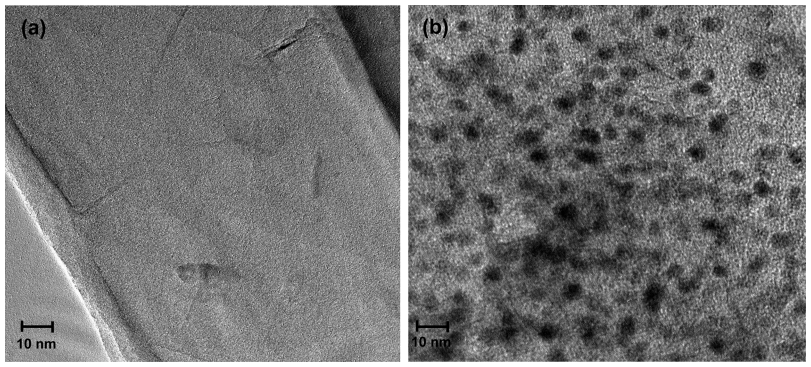

Figure 2. TEM images: (a) GO and (b) SPSGO.

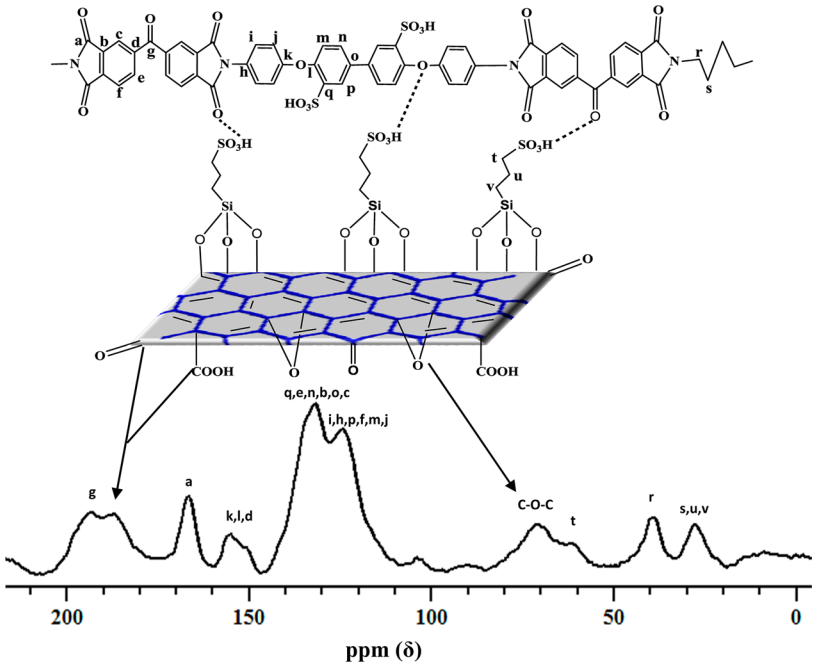

Figure 3. Solid-state ^{13}C NMR spectrum of SPI/SPSGO-8 composite membrane.

uptake, swelling ratio, and number of water molecules associated per ionic sites (λ) are included in section S2 of Supporting Information. Ion-exchange capacity (IEC) was measured by the back-titration method; detailed procedure is included in section S3 of Supporting Information. Procedures for studying oxidative and hydrolytic stabilities of the composite membranes are included in section S4 of Supporting Information.

Membrane Conductivity and Methanol Permeability. Membrane conductivity was measured in through-plane direction. Detailed procedures for measurement of proton conductivity and electronic conductivity are included in section S5 of Supporting Information. Methanol permeability of the composite membranes was determined in a diaphragm diffusion cell (see section S6 of Supporting Information).

Direct Methanol Fuel Cell Performance. Single-cell DMFC performance of prepared SPSGO/SPI composite membranes was compared with pristine membrane (SPI) and Nafion 117 with the help of a MTS-150 manual fuel cell test station (ElectroChem Inc.). Fuel cell test station was equipped with controlled fuel flow and pressure and temperature regulation attached with electronic load control ECL-150 (ElectroChem Inc.). For studying DMFC single-cell performance, the anode was made by coating a slurry of catalyst (50 wt % Pt + 50 wt % Ru on carbon), 5 wt % Nafion ionomer solution, 2-propanol, and Millipore water (catalyst ink) on gas diffusion layer at a loading of 5 mg·cm^{-2} Pt and Ru. The cathode was obtained by coating the same catalyst ink lacking Ru at the same loading.[37] Measurements were performed in the air mode of operation at 10 psi pressure with a 2 M methanol fede at the anode side with pressure 7 psi at 70 °C for a representative membrane.

3. RESULTS AND DISCUSSION

Structural Characterization of GO and SPSGO. GO was synthesized by modified Hummers method, and the presence of oxygenated functional groups (such as hydroxyl, carboxyl, carbonyl, and oxygen epoxide) was confirmed by the Fourier transform infrared (FT-IR) spectrum presented in Figure S1a (Supporting Information). Absorption bands at υ = 3403, 1720, 1620, and 1053 cm^{-1} were observed due to O−H stretching, C═O stretching, adsorbed water, and C−O stretching vibration, respectively.[38] SPSGO was prepared by the condensation reaction of GO and MPTMS followed by oxidation of mercapto groups, and its structure was confirmed by FT-IR and solid-state ^{13}C NMR spectrum. FT-IR spectrum of SPSGO showed an absorption band at υ = 2927 cm^{-1}, due to the presence of C−H stretching of methylene groups (Figure S1b, Supporting Information). Further absorption bands at υ = 1096 and 689 cm^{-1} were observed due to Si−O stretching and Si−C stretching, respectively. Absorption bands at υ = 1026

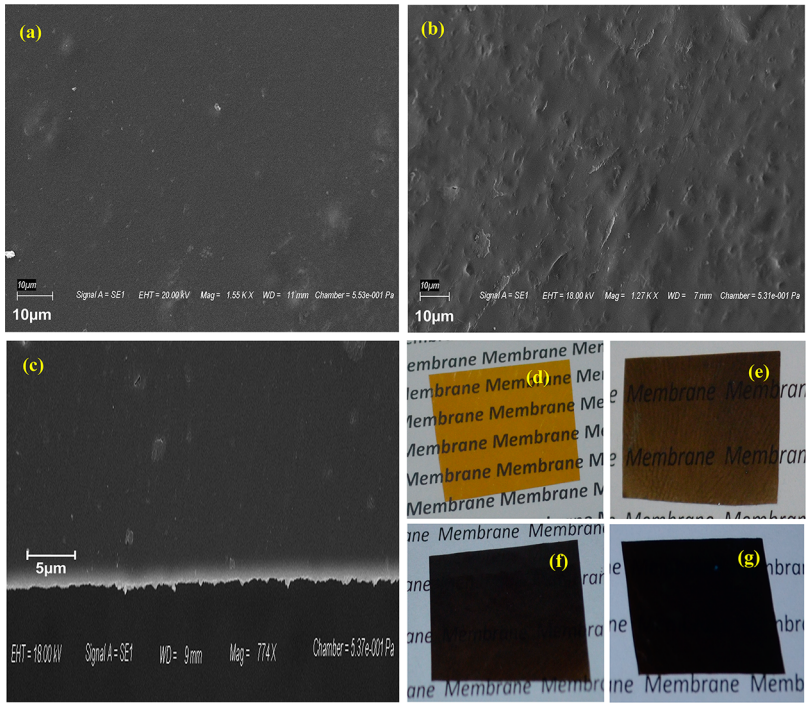

Figure 4. (a–c) SEM images: (a) SPI (surface), (b) SPI/SPSGO-8 (surface), and (c) SPI/SPSGO-8 (cross-section). (d–g) Optical images: (d) SPI, (e) SPI/SPSGO-4, (f) SPI/SPSGO-6, and (g) SPI/SPSGO-8.

(SO_2 symmetric stretch) and 1256 cm^{-1} (SO_2 asymmetric stretch) confirmed the oxidation of mercapto groups.[39,40] Solid-state ^{13}C NMR spectrum (Figure 1) showed a peak at 68.22 ppm due to the presence of epoxide carbon and peaks at 12.02, 25.38, and 41.34 ppm due to the presence of methylene carbon chain in SPSGO. The minor peaks at 129.36 and 168.35 ppm were assigned to aromatic functionalities (C═C) and to carbonyl carbons (C═O), respectively.[41,42]

TEM images of GO exhibited flat, exfoliated structure with some wrinkles (Figure 2a),[26] while TEM images of SPSGO showed some black dots on the surface, attributed to the clustering of sulfonic acid groups (Figure 2b). Presence of silica, sulfur, and oxygen on the surface of SPSGO was further confirmed by scanning transmission electron microscopy (STEM), elemental mapping images, and energy-dispersive spectroscopy (EDS) spectrum (Figure S2, Supporting Information).

SPI/SPSGO Composite Membrane. SPI/SPSGO composite membranes of different composition were prepared by solution casting in DMAc. The FT-IR spectrum of SPI/SPSGO composite membrane showed absorption bands at υ = 670 and 1088 cm^{-1}, due to the presence of Si–C and Si–O groups, respectively (Figure S1c, Supporting Information). Absorption bands at υ = 1021, 1166 (SO_2 symmetric stretch), and 1239 cm^{-1} (SO_2 asymmetric stretch) confirmed the presence of sulfonic acid groups in the membrane matrix. Peaks at υ = 1638, 1773, and 1705 cm^{-1} were attributed to the C═C bond stretching of phenol ring and symmetric and asymmetric stretching of C═O groups, respectively. The broad absorption band at υ = 3431 cm^{-1} was observed due to the strong hydrogen-bond interaction between SPI and SPSGO matrix. Solid-state ^{13}C NMR spectrum of SPI/SPSGO composite membrane showed all the expected peaks, clearly assigned in Figure 3.

SEM images of pristine SPI and SPI/SPSGO-8 composite membranes (Figure 4a,b) revealed the change in surface morphology after grafting of SPSGO with SPI. Pristine SPI membrane exhibited a smooth surface, while composite membrane showed a relatively rough surface. Cross-sectional image for SPI/SPSGO-8 composite membrane revealed homogeneous grafting of SPSGO in SPI matrix (Figure 4c). Pristine SPI membranes lost their transparency with progressive increase in SPSGO content in the membrane matrix Figure 4d–g.

The XRD spectrum of graphite (Gt) showed a diffraction peak at about 2θ = 26.39°, corresponding to the interplanar distance between the different graphene layers (Figure S3a, Supporting Information). Due to chemical oxidation of graphite, the order of graphene layers was disturbed and interlayer spacing between graphene sheets was increased. Thus, for GO, the value of the diffraction peak decreased to around 2θ = 11.80°, confirming the successful oxidation of graphite. Furthermore, broad diffraction peaks around 2θ = 11° and 20° for SPSGO also confirmed the successful modification of GO surface by MPTMS.[32]

The XRD pattern of pristine SPI membrane showed a peak at around 2θ = 22.98°, associated with the intricacy of an amorphous region and a crystalline region (Figure S3b, Supporting Information). The SPI/SPSGO-8 composite membrane showed a broad peak, due to strong interaction between SPI matrix and SPSGO. Broad peak at 11° corresponds to the filler (SPSGO). Thus, exfoliation of SPSGO layers in the SPI polymer matrix has been ruled out.

Thermal and Mechanical Properties. Thermogravimetric analysis curves for GO and SPSGO are compared in Figure S4 (Supporting Information). Below 150 °C, GO exhibited 13 wt % weight loss, while SPSGO showed 20 wt % weight loss, because of evaporation of adsorbed and bound water. Between 150 and 250 °C, GO exhibited 14 wt % weight loss, due to

decomposition of oxygen-containing functional groups (CO, CO_2, etc.), while 21 wt % weight loss for SPSGO was observed due to decomposition of carboxylic acid and sulfonic acid groups. Beyond 250 °C, 45.86−52.84 wt % weight loss was attributed to the disruption of graphene oxide layers.

Thermal stability of pristine SPI and SPI/SPSGO composite membranes was also compared with that of Nafion 117 membrane (Figure S5, Supporting Information). All membranes exhibited three-step weight loss. Below 150 °C, weight loss was observed due to evaporation of absorbed and bound water. Between 200 and 400 °C, weight loss was observed due to decomposition of oxygen-containing functional groups (CO, CO_2, SO_3H, etc.). Above 450 °C, weight loss was observed due to decomposition of polymer backbones, and in the case of different composite membranes, weight loss was reduced with increasing SPSGO content in the membrane matrix. Finally, values of 37.21 and 49.28 wt % remaining residues were obtained for pristine SPI and SPI/SPSGO-8 composite membrane. Thus, incorporation of SPSGO in the SPI matrix improved the thermal stability of composite membranes. At 750 °C, SPI/SPSGO-8 composite membrane showed 50.37 wt % residual mass, while only 7.70 wt % residual mass for Nafion 117 also revealed improved thermal stability of the former in comparison with the latter.

Mechanical stability of membranes was studied in terms of storage modulus via the dynamic mechanical analyzer (Figure S6, Supporting Information). The storage modulus of SPI matrix increased with the addition of SPSGO and afforded significant mechanical reinforcement. The SPI/SPSGO-8 membrane exhibited 2840 MPa storage modulus while pristine membrane exhibited 2238 MPa storage modulus at 30 °C. Compared with Nafion 117 membrane, SPI/SPSGO-8 composite membrane exhibited 9 times more storage modulus at 30 °C.

Oxidative and Hydrolytic Stability. Oxidative and hydrolytic stabilities of SPI/SPSGO composite membranes, in wet conditions, were extensively analyzed by recoding the weight loss under treatment with Fenton's reagent at 80 °C for 1 h and under pressurized steam at 140 °C for 24 h, respectively. Under both conditions, membranes were unbroken and showed about 0.98−2.29% weight loss (Table 1).

Table 1. Oxidative and Hydrolytic Stability of Different Composite Membranes

membrane	oxidative stability (% wt loss)	hydrolytic stability (% wt loss)
SPI	2.11 ± 0.5	0.98 ± 0.5
SPI/SPSGO-4	2.18 ± 0.5	1.14 ± 0.5
SPI/SPSGO-6	2.23 ± 0.5	1.19 ± 0.5
SPI/SPSGO-8	2.29 ± 0.5	1.26 ± 0.5

These data confirmed the oxidative and hydrolytic stable nature of SPI/SPSGO composite membranes may be due to strong hydrogen-bonding interactions between SPSGO and sulfonic acid groups of SPI matrix.

Water Uptake, Swelling Ratio, Ion-Exchange Capacity, and State of Water. Incorporation of nonconducting materials (such as TiO_2, SiO_2, graphene, etc.) into ionic conducting SPI matrix would lower the proton conductivity and IEC. To avoid this deterioration, GO was functionalized into SPSGO by grafting of -SO_3H groups and incorporated into SPI matrix for developing PEM with improved conductivity and IEC. Water uptake (WU), swelling ratio, and IEC (Table 2) are the important parameters in determining the hydrophilic nature of the membranes. Pristine SPI and GO-incorporated composite membrane (SPI/GO-8) showed relatively low WU values. The WU values for SPI/SPSGO composite membranes increased with SPSGO content, which may be due to increased density of hydrophilic functional groups. Swelling properties of pristine SPI membrane altered markedly after incorporation of GO/SPSGO (Table 2). Incorporation of GO into SPI matrix reduced its swelling behavior, while functionalized SPSGO enhanced the swelling behavior. Improved swelling behavior of SPI/SPSGO composite membrane was attributed to the highly hydrophilic membrane surface due to high density of sulfonic/carboxylic acid groups in SPSGO. Thus, it is necessary to study the trade-off behavior of composite membranes by varying the content of membrane-forming material and properties.

IEC values of composite membranes increased with SPSGO content in membrane matrix, and SPI/SPSGO composite membranes showed high IEC values in comparison with Nafion 117 membrane (0.90 mequiv·g^{-1}) (Table 2). This observation also supports the aforementioned statements. Alternatively, the values depicted in Table 2 were increased with incorporation of SPSGO content to SPI matrix, and SPI/SPSGO-8 composite membrane showed 15.12 water molecules per ionic site (λ), responsible for formation of ionic clusters in the membrane matrix. In the case of Nafion 117 membrane, a value of about 25.68 water molecules per ionic site was found.

Water-Retention Ability of SPI/SPSGO Composite Membranes. Water-retention ability of PEM plays an important role for proton conduction at elevated temperature (>100 °C). PEM possess two types of water: bound water and bulk water. Bound water is required for solvation of the acidic groups, while bulk water fills the void volume.[43] For easy comparison, weight loss percentages for different membrane samples were fixed at 100% at 100 °C (Figure S7, Supporting Information). Pristine SPI and Nafion 117 membrane showed the lowest and comparable water retaining ability with 0.62% and 1.04% bound water content, respectively (Table 3). Among the SPI/SPSGO composite membranes, 6.58% bound water content for SPI/SPSGO-8 membrane confirmed the enhanced

Table 2. Water Uptake, Ion-Exchange Capacity, Swelling Ratio, and Number of Water Molecules per Ionic Site for Different Membranes

membrane	WU (%)	IEC (mequiv/g)	swelling ratio (%) at 65 °C	λ
SPI	31.31 ± 0.3	1.77 ± 0.05	10.56 ± 0.2	9.82 ± 0.2
SPI/GO-8	30.20 ± 0.3	1.71 ± 0.05	8.19 ± 0.2	9.81 ± 0.2
SPI/SPSGO-4	45.04 ± 0.3	1.83 ± 0.05	11.28 ± 0.2	13.67 ± 0.2
SPI/SPSGO-6	49.28 ± 0.3	1.89 ± 0.05	12.86 ± 0.2	14.48 ± 0.2
SPI/SPSGO-8	55.82 ± 0.3	2.05 ± 0.05	13.29 ± 0.2	15.12 ± 0.2
Nafion 117	41.60 ± 0.3	0.90 ± 0.05	15.05 ± 0.2	25.68 ± 0.2

Table 3. Total, Bulk, and Bound Water Content of Different Composite Membranes and Nafion 117 Membrane

membrane	total water (%)	bulk water[a] (%)	bound water[b] (%)
SPI	31.31 ± 0.3	30.69 ± 0.2	0.62 ± 0.1
SPI/GO-8	30.20 ± 0.3	28.98 ± 0.2	1.22 ± 0.1
SPI/SPSGO-4	45.04 ± 0.3	41.06 ± 0.2	3.98 ± 0.1
SPI/SPSGO-6	49.28 ± 0.3	44.41 ± 0.2	4.87 ± 0.1
SPI/SPSGO-8	55.82 ± 0.3	49.24 ± 0.2	6.58 ± 0.1
Nafion 117	41.60 ± 0.3	40.56 ± 0.2	1.04 ± 0.1

[a]Bulk water = total water − bound water. [b]Bound water was determined by percent weight loss in TGA between 100 and 150 °C.

bound water content of the SPI matrix due to incorporation of SPSGO. High bound water content of composite membranes improved their water-retaining ability and thus proton conductivity under low-humidity conditions.

Water vapor sorption and diffusion properties of PEMs showed a profound effect on their conductivity and suitability for fuel applications. The water-retention capability of SPI/SPSGO composite membranes has been illustrated in Figure S8a (Supporting Information) by M_t/M_0 versus t (time) curves. Deswelling kinetics of these composite membranes was further characterized by M_t/M_0 versus $t^{1/2}$ curves (Figure S8b, Supporting Information) by use of Higuchi's model:[44]

$$M_t/M_0 = -kt^{1/2} + 1 \quad (1)$$

where M_0 is the initial amount of water, M_t is the amount of water remaining in polymer matrix at any given time t, and k is a constant. For different composite membranes with varied content of SPSGO, obtained straight lines were fitted to Higuchi's model, which suggested a diffusion-controlled water desorption mechanism. SPSGO possesses a high density of functional groups, responsible for the formation of bound water-filled ionic clusters in the membrane matrix. Because of more bound water, the polymer matrix was less opting to dehydration. Thus, SPSGO acted as a barrier for water release and improved the water-retention capacity even at higher temperature.

Conductivity and Methanol Permeability. Acidic functional groups (-SO_3H and -COOH) of composite PEM membranes dissociate due to hydration and allow transport of hydrated proton (H_3O^+). Proton conductivity (κ^m) is an important parameter to assess the suitability of a membrane for PEM fuel cell applications. The κ^m values at 30 °C for SPI, SPI/GO, and SPI/SPSGO composite membranes are included in Table 4. Incorporation of SPSGO in SPI matrix improved the proton conductivity, perhaps due to formation of interconnected proton conducting channels (Scheme 2). SPI/GO-8 membrane showed 7.19×10^{-2} S·cm^{-1} membrane conductivity, while the corresponding value for pristine SPI membrane was 6.04×10^{-2} S·cm^{-1}. This may be attributed to the absence of sulfonic acid groups in GO. Accordingly, IEC values for pristine SPI (1.77 mequiv/g) and SPI/GO-8 membrane (1.71 mequiv/g) support this observation. Also, proton conductivity of pristine SPI membrane (6.04×10^{-2} S·cm^{-1}) was markedly improved to 9.62×10^{-2} S·cm^{-1} for SPI/SPSGO-8 membrane (nearly equal to proton conductivity of Nafion 117 membrane).

Temperature dependence (30−90 °C) of κ^m for prepared membranes showed consistency with the Arrhenius relationship (Figure 5). Activation energy (E_a), the minimum energy

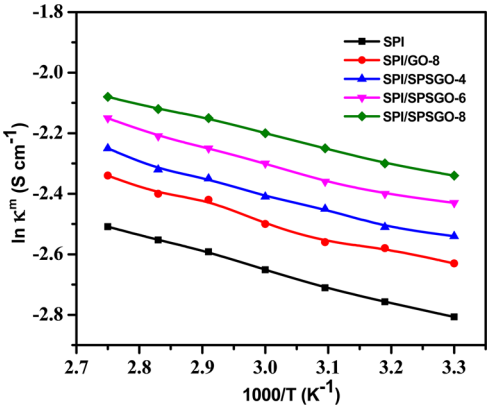

Figure 5. Arrhenius plots of different composite membranes (error limit ±0.3%).

required for proton conduction, varied from 4.57 to 4.03 kJ·mol^{-1} for pristine SPI and composite membranes. Incorporation of SPSGO in the SPI matrix moderately reduced the activation energy values (Table 4). These data confirmed relatively easy proton conduction across SPI/SPSGO membranes.

Very small loading of GO to add electron conductivity to polymer insulators is well-known. Conductivity values depend on the composition and characteristics of GO, like aspect ratio and surface functionalization (Table 4). Data revealed that electron conductivity of pristine SPI jumped about 4-fold after incorporation of GO (SPI/GO-8 membrane). After functionalization (with SPSGO), the increase of electronic conductivity relative to pristine SPI was only about 2−3-fold, depending on composition. But these values are low in comparison with that obtained without functionalization. The electrical property of GO is known to be very dependent on structural changes caused by chemical treatment and may be due to partial disturbance of π-conjugated sp^2 carbon bonds.

Membrane permeability (P) depends on the nature of the membrane-forming material and operating conditions of the

Table 4. Proton Conductivity,[a] Electronic Conductivity, Selectivity Parameter,[a,b] and Activation Energy for Different Composite Membranes and Nafion 117 Membrane

membrane	$\kappa^m \times 10^{-2}$ (S·cm^{-1})	electronic conductivity $\times 10^{-9}$ (S·cm^{-1})	SP $\times 10^4$ (S·cm^{-3} ·s)	E_a (kJ·mol^{-1})
SPI	6.04 ± 0.01	1.74 ± 0.3	4.13 ± 0.05	4.57 ± 0.2
SPI/GO-8	7.19 ± 0.01	6.87 ± 0.3	5.32 ± 0.05	4.44 ± 0.2
SPI/SPSGO-4	7.88 ± 0.01	3.51 ± 0.3	5.55 ± 0.05	4.37 ± 0.2
SPI/SPSGO-6	8.81 ± 0.01	4.76 ± 0.3	6.43 ± 0.05	4.30 ± 0.2
SPI/SPSGO-8	9.62 ± 0.01	5.92 ± 0.3	7.34 ± 0.05	4.03 ± 0.2
Nafion 117	9.56 ± 0.01		3.73 ± 0.05	5.45 ± 0.2

[a]Testing temperature 30 °C. [b]Measured in 8 M methanol.

fuel cell, such as temperature, feed composition, and pressure. When GO was added to the SPI matrix, methanol permeability was reduced (Figure 6). However, without functionalization by

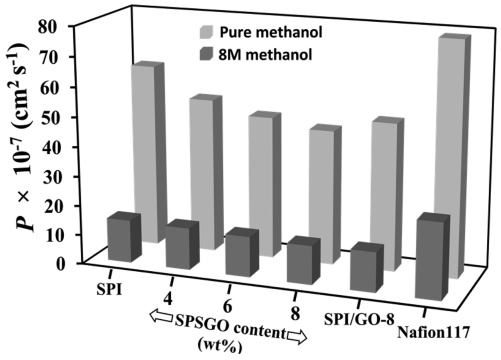

Figure 6. Methanol permeability (P) of composite membranes in pure and 8 M methanol at 30 °C (error limit ±0.1%).

GO, the weak adhesion between polymer matrix and nanofillers gives rise to cavities, which favor molecular diffusion. With functionalization, the membrane's void volume was reduced because of strong H-bonding. This is further leading to much slower diffusion of the penetrants and low permeability. Methanol permeability of the pristine SPI membrane for 8 M methanol at 30 °C (14.6×10^{-7} $cm^2 \cdot s^{-1}$) was reduced to 13.1 $\times$ 10^{-7} $cm^2 \cdot s^{-1}$ in the case of SPI/SPSGO-8 composite membrane. As a reference, methanol permeability of SPI/SPSGO-8 membrane was quite low in comparison with Nafion 117 membrane under similar experimental conditions. Membrane separation performance depends on the interaction between species to be diffused and on the membrane matrix. Hydrophilic membranes like SPI/SPSGO composite developed H-bond interaction with methanol/water, leading to their preferential sorption and permeation of water through the membrane.

The ratio between proton conductivity and methanol permeability (κ^m/P) is known as the selectivity parameter (SP) (Table 4). The SP value for pristine SPI membrane (4.13×10^4 $S \cdot cm^{-3} \cdot s$) increased to 7.34×10^4 $S \cdot cm^{-3} \cdot s$ for SPI/SPSGO-8 membrane. Furthermore, SPI/SPSGO-8 membrane exhibited about 1.60-fold greater values than that for Nafion 117 membrane. This may be attributed to improved proton conductivity and reduced methanol permeability of SPI/SPSGO composite membrane, in comparison with pristine SPI membrane. Ionized groups hydrate strongly and exclude organic solvents (salting-out effect), which is an essential feature for the PEM and indicates a great advantage for DMFC applications.

Direct Methanol Fuel Cell Performance Studies. Figure 7a shows single-cell DMFC performance for SPI/SPSGO composite membranes, pristine SPI membrane, and Nafion 117 membrane. Polarization curves (current density as a function of cell potential and power density) were recorded with 2 M methanol as the fuel at 70 °C. SPI/SPSGO-8 membrane showed high open-circuit voltage (OCV) (0.70 V) in comparison with Nafion 117 (0.68 V). At 0.2 V applied voltage, SPI, SPI/GO-8, SPI/SPSGO-8, and Nafion 117 membranes showed 165, 194, 334, and 270 $mA \cdot cm^{-2}$ current densities, respectively. These data confirmed comparable DMFC performance of SPI/SPSGO-8 composite and Nafion 117 membrane. Furthermore, after incorporation of SPSGO in

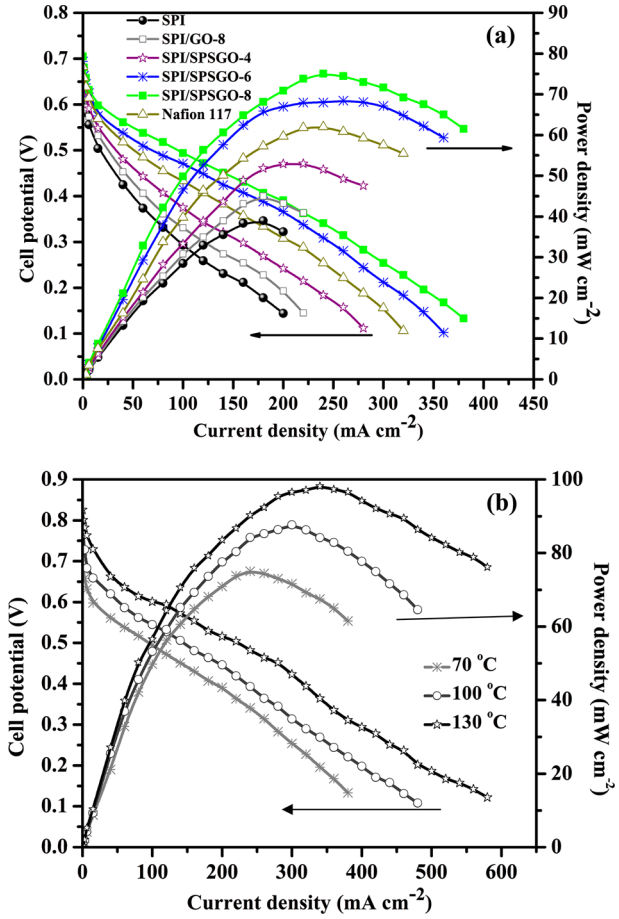

Figure 7. (a) Direct methanol fuel cell tests curves for SPI/SPSGO composite membranes and Nafion 117 membrane with 2 M methanol at 70 °C (error limit ±0.5%). (b) Polarization and power density of single cells employing a SPI/SPSGO-8 membrane with 2 M methanol at different temperatures.

SPI matrix, cell performance was clearly improved in comparison with pristine SPI membrane. The maximum power density for SPI/SPSGO-8 composite membrane (75.06 $mW \cdot cm^{-2}$) indicated comparable DMFC performance to Nafion 117 membrane (62.40 $mW \cdot cm^{-2}$). Also, the result of methanol permeability of SPI/SPSGO-8 membrane makes it possible to operate the single-cell tests with methanol fuel in high concentrations. Increase in operating temperature is beneficial for DMFC operation. In the case of SPI/SPSGO-8 membrane, maximum power output of the cell, 75.06 $mW \cdot cm^{-2}$ at 70 °C, increased to 98.18 $mW \cdot cm^{-2}$ at 130 °C (Figure 7b). In addition, DMFC performance with SPI/SPSGO-8 membrane was studied for 70 h by recording the current density (Figure 8). The cell with SPI/SPSGO-8 membrane showed reasonable stability with a gradual drop in current density (0.27 $mA \cdot h^{-1}$ degradation rate) over the test period. These studies confirmed reasonable stability of the cell with prepared SPI/SPSGO-8 membrane.

CONCLUSIONS

We successfully functionalized GO by grafting -SO_3H groups. SPI/SPSGO composite PEMs were fabricated and characterized. Loading of acidic functionalized GO (SPSGO) in the SPI matrix influenced different desirable membrane properties relevant for DMFC applications (Figure 9). The most suitable

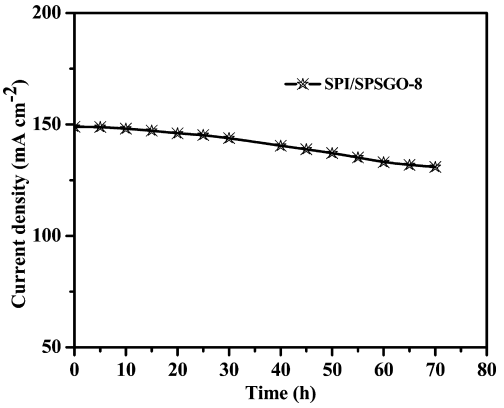

Figure 8. Cell stability measured at 0.6 V cell potential and 100 °C in 2 M methanol/air.

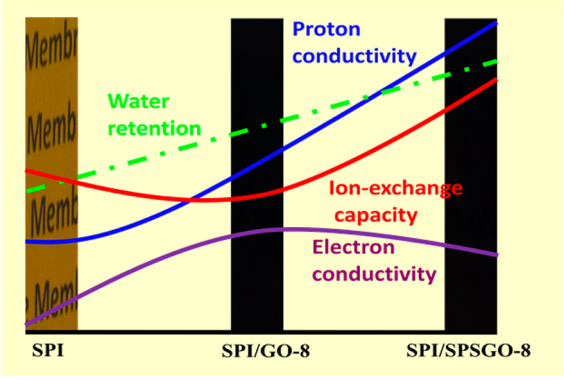

Figure 9. Influence of GO and SPSGO on different desirable membrane properties.

assessed PEM (SPI/SPSGO-8) contained 8 wt % SPSGO, and the following effects were obtained: (1) improvement in membrane stabilities and about 10-fold enhanced bound water content; (2) improvement in proton conductivity from 6.0 to 9.62 $S \cdot cm^{-1}$ (nearly equal to that for Nafion 117); (3) marginal jump in electron conductivity (about 3-fold); and (4) marginal reduction of methanol permeability in comparison with pristine SPI membrane.

The content of SPSGO in SPI matrix not only promoted proton conductivity but also improved the mechanical and thermal stabilities along with bound water content, responsible for slow dehydration of the membrane matrix. The composite membranes were designed to promote internal self-humidification responsible for water-retention properties and to promote proton conduction due to the presence of different acidic functional groups. Strong H-bonding between the functional groups and presence of hydrophobic graphene sheets and polymer chains provides a suitable architecture of proton conducting channels in the membrane matrix. Single-cell DMFC performance of SPI/SPSGO composite membranes also confirmed the suitability of optimized SPI/SPSGO-8 membrane for DMFC applications.

However, several limitations, including lifetime of the membrane electrode assembly of the proposed PEMs, have to be overcome before commercial exploitation is feasible. Nevertheless, proposed results showed significant scope for the simple designing of nonfluorinated PEM with better performance.

■ ASSOCIATED CONTENT

Ⓢ Supporting Information

Six text sections with details of chemical, structural, and physiochemical characterization and membrane stability; eight figures showing FT-IR spectra, STEM and EDS mapping, XRD patterns, TGA curves, DMA analysis, bound water content, and water desorption profiles. This material is available free of charge via the Internet at http://pubs.acs.org/.

■ AUTHOR INFORMATION

Corresponding Author

*Fax +91-0278-2566970; tel +91-278-2569445; e-mail vkshahi@csmcri.org or vinodshahi1@yahoo.com.

Notes

The authors declare no competing financial interest.

■ ACKNOWLEDGMENTS

CSIR-CSMCRI Registration number 161/2014. R.P.P. is thankful to University Grand Commission (UGC), New Delhi, for providing a senior research fellowship (SRF). This work is supported by Ministry of New and Renewable Energy Sources (Project 102/79/2010-NT), Government of India. Instrumental support received from Analytical Science Division, CSMCRI, is also gratefully acknowledged.

■ REFERENCES

(1) Maab, H.; Schieda, M.; Yave, W.; Shishatskiy, S.; Nunes, S. P. SPEEK/Polyimide Blends for Proton Conductive Membranes. *Fuel Cells* **2009**, *9*, 401−409.

(2) Tripathi, B. P.; Schieda, M.; Shahi, V. K.; Nunes, S. P. Nanostructured Membranes and Electrodes with Sulphonic Acid Functionalized Carbon Nanotubes. *J. Power Sources* **2011**, *196*, 911−919.

(3) Jacobson, M. Z.; Colella, W. G.; Golden, D. M. Cleaning the Air and Improving Health with Hydrogen Fuel-Cell Vehicles. *Science* **2005**, *308*, 1901−1905.

(4) Tian, Z. Q.; Lim, S. H.; Poh, C. K.; Tang, Z.; Xia, Z.; Luo, Z.; Shen, P. K.; Chua, D.; Feng, Y. P.; Shen, Z.; Lin, J. A Highly Order-Structured Membrane Electrode Assembly with Vertically Aligned Carbon Nanotubes for Ultra-Low Pt Loading PEM Fuel Cells. *Adv. Energy Mater.* **2011**, *1*, 1205−1214.

(5) Li, L.; Zhang, J.; Wang, Y. Sulphonated Poly(ether ether ketone) Membranes for Direct Methanol Fuel Cell. *J. Membr. Sci.* **2013**, *226*, 159−167.

(6) Li, Q.; He, R.; Jensen, J. O.; Bjerrum, N. J. Approaches and Recent Development of Polymer Electrolyte Membranes for Fuel Cells Operating above 100 °C. *Chem. Mater.* **2003**, *15*, 4896−4915.

(7) Tripathi, B. P.; Chakrabarty, T.; Shahi, V. K. Highly Charged and Stable Cross-linked 4,4′-Bis(4-aminophenoxy)biphenyl-3,3′-disulfonic Acid (BAPBDS)-Sulphonated poly(ether sulfone) Polymer Electrolyte Membranes Impervious to Methanol. *J. Mater. Chem.* **2010**, *20*, 8036−8044.

(8) Hickner, M. A.; Ghassemi, H.; Kim, Y. S.; Einsla, B. R.; McGrath, J. E. Alternative Polymer Systems for Proton Exchange Membranes (PEMs). *Chem. Rev.* **2004**, *104*, 4587−4612.

(9) Peckham, T. J.; Holdcroft, S. Structure-Morphology-Property Relationships of Non-Perfluorinated Proton-Conducting Membranes. *Adv. Mater.* **2010**, *22*, 4667−4690.

(10) Chai, Z.; Wang, C.; Zhang, H.; Doherty, C. M.; Ladewig, B. P.; Hill, A. J.; Wang, H. Nafion−Carbon Nanocomposite Membranes Prepared Using Hydrothermal Carbonization for Proton-Exchange-Membrane Fuel Cells. *Adv. Funct. Mater.* **2010**, *20*, 4394−4399.

(11) Miyatake, K.; Tombe, T.; Chikashige, Y.; Uchida, H.; Watanabe, M. Enhanced Proton Conduction in Polymer Electrolyte Membranes with Acid-Functionalized Polysilsesquioxane. *Angew. Chem., Int. Ed.* **2007**, *46*, 6646−6649.

(12) Dong, B.; Gwee, L.; Cruz, D. S.; Winey, K. I.; Elabd, Y. A. Super Proton Conductive High-Purity Nafion Nanofibers. *Nano Lett.* **2010**, *10*, 3785−3790.
(13) Kannan, R.; Kakade, B. A.; Pillai, V. K. Polymer Electrolyte Fuel Cells Using Nafion-Based Composite Membranes with Functionalized Carbon Nanotubes. *Angew. Chem., Int. Ed.* **2008**, *47*, 2653−2656.
(14) Casciola, M.; Alberti, G.; Sganappa, M.; Narducci, R. On the Decay of Nafion Proton Conductivity at High Temperature and Relative Humidity. *J. Power Sources* **2006**, *162*, 141.
(15) Bae, B.; Yoda, T.; Miyatake, K.; Uchida, H.; Watanabe, M. Proton-Conductive Aromatic Ionomers Containing Highly Sulphonated Blocks for High-Temperature-Operable Fuel Cells. *Angew. Chem., Int. Ed.* **2010**, *49*, 317−320.
(16) Tripathi, B. P.; Shahi, V. K. Organic−Inorganic Nanocomposite Polymer Electrolyte Membranes for Fuel Cell Applications. *Prog. Polym. Sci.* **2011**, *36*, 945−979.
(17) Meyer, G.; Gebel, G.; Gonon, L.; Capron, P.; Marscaq, D.; Marestin, C.; Marcier, R. Degradation of Sulphonated Polyimide Membranes in Fuel Cell Conditions. *J. Power Sources* **2006**, *157*, 293−301.
(18) Chen, K. C.; Hu, Z. X.; Endo, N.; Higa, M.; Okamoto, K.-I. Sulphonated Multiblock Copolynaphthalimides for Polymer Electrolyte Fuel Cell Application. *Polymer* **2011**, *52*, 2255−2262.
(19) Miyatake, K.; Zhou, H.; Uchida, H.; Watanabe, M. Highly Proton Conductive Polyimide Electrolytes Containing Fluorenyl Groups. *Chem. Commun.* **2003**, 368−369.
(20) Li, N.; Cui, Z.; Zhang, S.; Li, S.; Zhang, F. Preparation and Evaluation of a Proton Exchange Membrane Based on Oxidation and Water Stable Sulphonated Polyimides. *J. Power Sources* **2007**, *172*, 511−519.
(21) Pandey, R. P.; Shahi, V. K. Aliphatic-Aromatic Sulphonated Polyimide and Acid Functionalized Polysilsesquioxane Composite Membranes for Fuel Cell Applications. *J. Mater. Chem. A* **2013**, *1*, 14375−14383.
(22) Tseng, C.-Y.; Ye, Y.-S.; Cheng, M.-Y.; Kao, K.-Y.; Shen, W.-C.; Rick, J.; Chen, J.-C.; Hwang, B.-J. Sulphonated Polyimide Proton Exchange Membranes with Graphene Oxide show Improved Proton Conductivity, Methanol Crossover Impedance, and Mechanical Properties. *Adv. Energy Mater.* **2011**, *1*, 1220−1224.
(23) Dikin, D. A.; Stankovich, S.; Zimney, E. J.; Piner, R. D.; Dommett, G. H. B.; Evmenenko, G.; Nguyen, S. T.; Ruoff, R. S. Preparation and Characterization of Graphene Oxide Paper. *Nature* **2007**, *448*, 457−460.
(24) McAllister, M. J.; Li, J.-L.; Adamson, D. H.; Schniepp, H. C.; Abdala, A. A.; Liu, J.; Alonso, M. H.; Milius, D. L.; Car, R.; Prud'homme, R. K.; Aksay, I. A. Single Sheet Functionalized Graphene by Oxidation and Thermal Expansion of Graphite. *Chem. Mater.* **2007**, *19*, 4396−4404.
(25) Cerveny, S.; Bujans, F. B.; Alegria, A.; Colmenero, J. Dynamics of Water Intercalated in Graphite Oxide. *J. Phys. Chem. C* **2010**, *114*, 2604−2612.
(26) Zarrin, H.; Higgins, D.; Jun, Y.; Chen, Z.; Fowler, M. Functionalized Graphene Oxide Nanocomposite Membrane for Low Humidity and High Temperature Proton Exchange Membrane Fuel Cells. *J. Phys. Chem. C* **2011**, *115*, 20774−20781.
(27) Hantel, M. M.; Kaspar, T.; Nesper, R.; Wokaun, A.; Kotz, R. Partially Reduced Graphite Oxide for Supercapacitor Electrodes: Effect of Graphene Layer Spacing and Huge Specific Capacitance. *Electrochem. Commun.* **2011**, *13*, 90−92.
(28) Kumar, R.; Xu, C.; Scott, K. Graphite Oxide/Nafion Composite Membranes for Polymer Electrolyte Fuel Cells. *RSC Adv.* **2012**, *2*, 8777−8782.
(29) Zhang, J.; Zhang, F.; Yang, H.; Huang, X.; Liu, H.; Zhang, J.; Guo, S. Graphene Oxide as a Matrix for Enzyme Immobilization. *Langmuir* **2010**, *26*, 6083−6085.
(30) Karim, M. R.; Hatakeyama, K.; Matsui, T.; Takehira, H.; Taniguchi, T.; Koinuma, M.; Matsumoto, Y.; Akutagawa, T.; Nakamura, T.; Noro, S.-I.; Yamada, T.; Kitagawa, H.; Hayami, S. Graphene Oxide Nanosheet with High Proton Conductivity. *J. Am. Chem. Soc.* **2013**, *135* (22), 8097−8100.
(31) Jiang, Z.; Zhao, X.; Manthiram, A. Sulphonated Poly(ether ether ketone) Membranes with Sulphonated Graphene Oxide Fillers for Direct Methanol Fuel Cells. *Int. J. Hydrogen Energy* **2013**, *38*, 5875−5884.
(32) Kumar, R.; Scott, K. Freestanding Sulphonated Graphene Oxide Paper: A New Polymer Electrolyte for Polymer Electrolyte Fuel Cells. *Chem. Commun.* **2012**, *48*, 5584−5586.
(33) Chien, H.-C.; Tsai, L.-D.; Huang, C.-P.; Kang, C.-y.; Lin, J.-N.; Chang, F.-C. Sulfonated Graphene Oxide/Nafion Composite Membranes for High-Performance Direct Methanol Fuel Cells. *Int. J. Hydrogen Energy* **2013**, *38*, 13792−13801.
(34) Lee, D. C.; Yang, H. N.; Park, S. H.; Kim, W. J. Nafion/Graphene Oxide Composite Membranes for Low Humidifying Polymer Electrolyte Membrane Fuel Cell. *J. Membr. Sci.* **2014**, *452*, 20−28.
(35) Yoonessi, M.; Shi, Y.; Scheiman, D. A.; Lebron-Colon, M.; Tigelaar, D. M.; Weiss, R. A.; Meador, M. A. Graphene Polyimide Nanocomposites; Thermal, Mechanical, and High-Temperature Shape Memory Effects. *ACS Nano* **2012**, *6* (9), 7644−7655.
(36) Zhang, Y.; Zhang, H.; Zhu, X.; Bi, C. Promotion of PEM Self-Humidifying Effect by Nanometer-Sized Sulfated Zirconia-Supported Pt Catalyst Hybrid with Sulphonated Poly(Ether Ether Ketone). *J. Phys. Chem. B* **2007**, *111*, 6391−6399.
(37) Li, H.-Y.; Liu, Y.-L. Nafion-Functionalized Electrospun Poly(vinylidene fluoride) (PVDF) Nanofibers for High Performance Proton Exchange Membranes in Fuel Cells. *J. Mater. Chem. A* **2014**, *2*, 3783−3793.
(38) Jiang, Z.; Zhao, X.; Fu, Y.; Manthiram, A. Composite Membranes Based on Sulphonated Poly(ether ether ketone) and SDBS-Adsorbed Graphene Oxide for Direct Methanol Fuel Cells. *J. Mater. Chem.* **2012**, *22*, 24862−24869.
(39) Pandey, R. P.; Shahi, V. K. Functionalized Silica−Chitosan Hybrid Membrane for Dehydration of Ethanol/Water Azeotrope: Effect of Cross-Linking on Structure and Performance. *J. Membr. Sci.* **2013**, *444*, 116−126.
(40) Singh, A. K.; Pandey, R. P.; Jasti, A.; Shahi, V. K. Self-Assembled Silica Nanocrystal-Based Anti-Biofouling Nanofilter Membranes. *RSC Adv.* **2013**, *3*, 458−467.
(41) Cai, W.; Piner, R. D.; Stadermann, F. J.; Park, S.; Shaibat, M. A.; Ishii, Y.; Yang, D.; Velamakanni, A.; An, S. J.; Stoller, M.; An, J.; Chen, D.; Ruoff, R. S. Synthesis and Solid-State NMR Structural Characterization of ^{13}C-Labeled Graphite Oxide. *Science* **2008**, *321*, 1815−1817.
(42) Szabó, T.; Berkesi, O.; Forgó, P.; Josepovits, K.; Sanakis, Y.; Petridis, D.; Dékány, I. Evolution of Surface Functional Groups in a Series of Progressively Oxidized Graphite Oxides. *Chem. Mater.* **2006**, *18*, 2740−2749.
(43) Eikerling, M.; Kornyshev, A. A.; Stimming, U. Electrophysical Properties of Polymer Electrolyte Membranes: A Random Network Model. *J. Phys. Chem. B* **1997**, *101*, 10807−10820.
(44) Liu, T. Y.; Chen, S. Y.; Lin, Y. L.; Liu, D. M. Synthesis and Characterization of Amphiphatic Carboxymethyl-hexanoyl Chitosan Hydrogel: Water-Retention Ability and Drug Encapsulation. *Langmuir* **2006**, *22*, 9740−9745.